

## Supporting Information

—

### **Unveiling the metal-dependent aggregation properties of the C-terminal region of amyloidogenic intrinsically disordered protein isoforms DPF3b and DPF3a**

Tanguy Leyder<sup>1,†</sup>, Julien Mignon<sup>1,2,3,†</sup>, Denis Mottet<sup>4</sup>, and Catherine Michaux<sup>1,2,3,\*</sup>

<sup>1</sup>*Laboratoire de Chimie Physique des Biomolécules, UCPTS, University of Namur, 61 rue de Bruxelles, 5000 Namur, Belgium*

<sup>2</sup>*Namur Institute of Structured Matter (NISM), University of Namur, Namur, Belgium*

<sup>3</sup>*Namur Research Institute for Life Sciences (NARILIS), University of Namur, Namur, Belgium*

<sup>4</sup>*GIGA-Molecular Biology of Diseases, University of Liège, Quartier Hôpital, Avenue de l'Hôpital 11, 4000 Liège, Belgium*

\*Corresponding author: Catherine Michaux, Laboratoire de Chimie Physique des Biomolécules, UCPTS, Université de Namur, rue de Bruxelles 61, 5000 Namur, Belgique.

Phone number: +32 81724557. E-mail address: catherine.michaux@unamur.be

<sup>†</sup>These authors contributed equally to this study

## C-TERb:

	200	210	220	230	240	250	260	270
	C	DICGKRYKNR	PGLSYHYAHT	HLASEEGDEA	QDQETRSPN	HRNENHRPQK	GPDGTVIPNN	YCDFCLGGSN
280	290	300	310	320	330	340	350	360
MNKKSGRPEE	LVSCADCGRS	GHPTCLQFTL	NMTEAVKTYK	WQCIECKSCI	LCGTSENDQ	LLFCDDCDRG	YHMYCLNPPV	AEPPEGWSW
370								
HLCWELLKEK	ASAFGCQA							

## C-TERa:

	200	210	220	230	240	250	260	270
	C	DICGKRYKNR	PGLSYHYAHT	HLASEEGDEA	QDQETRSPN	HRNENHRPQK	GPDGTVIPNN	YCDFCLGGSN
280	290	300	310	320	330	340	350	
MNKKSGRPEE	LVSCADCGRS	AHLGGEGRKE	KEAAAAARTT	EDLFGSTSES	DTSTFHGFDE	DDLEEPRSCR	GRRSGRGSPT	ADKKGSC

Figure S1 – Sequence composition of C-TERb (upper panel) and C-TERa (lower panel).

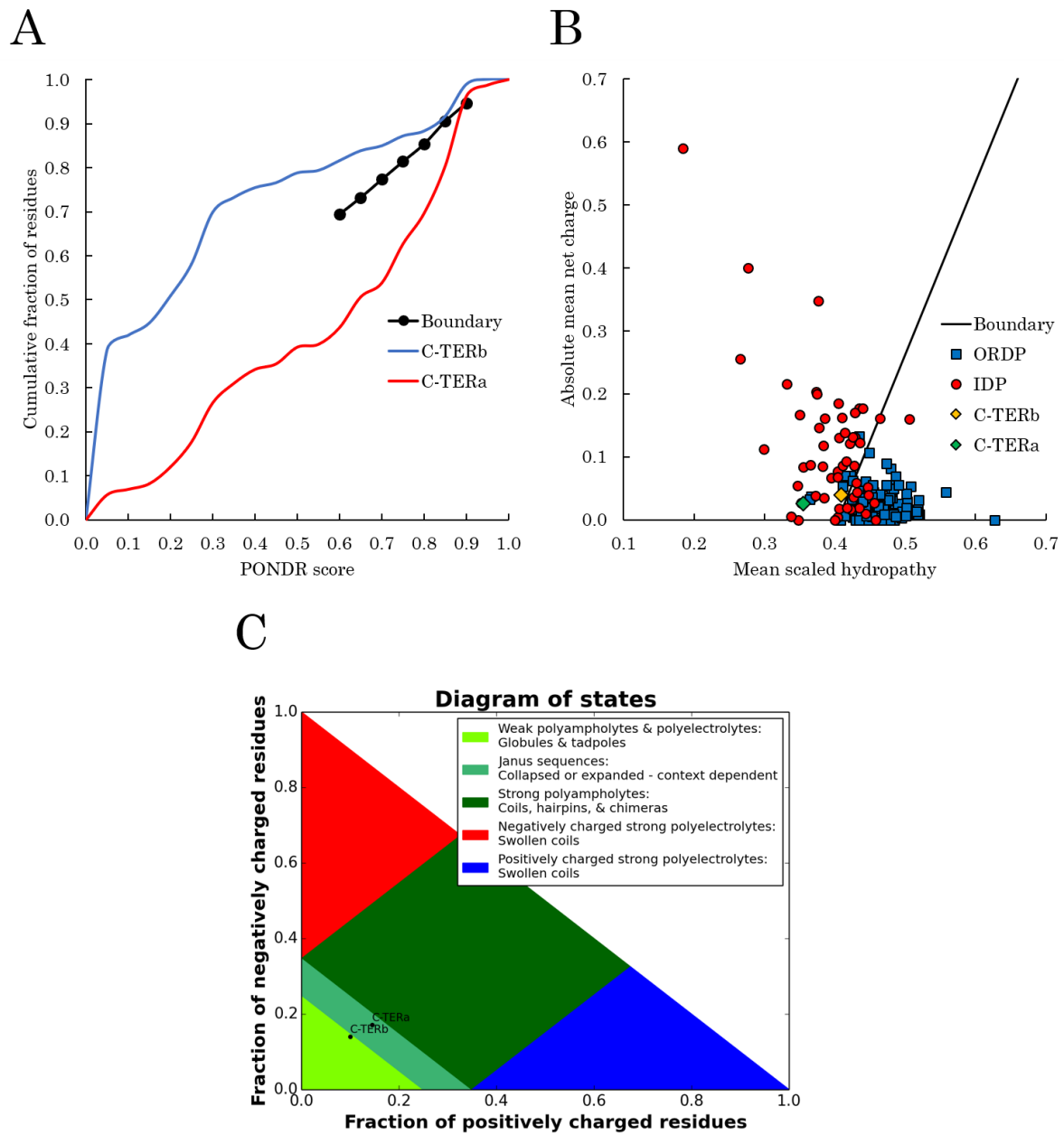


Figure S2 – Predicted disorder-associated properties of C-TERb and C-TERa. (A) CDF plot, (B) CH plot, and (C) Das-Pappu phase diagram.

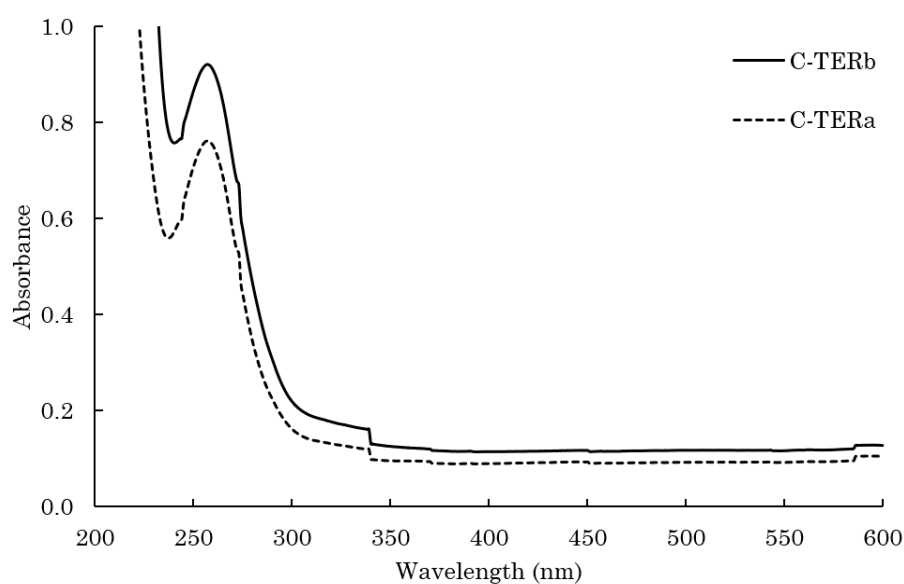


Figure S3 – UV-visible absorption spectra of C-TERb (solid line) and C-TERa (dashed line) in TBS at  $\sim 20^\circ\text{C}$  ( $C_{\text{C-TER}} = 10\ \mu\text{M}$ ).

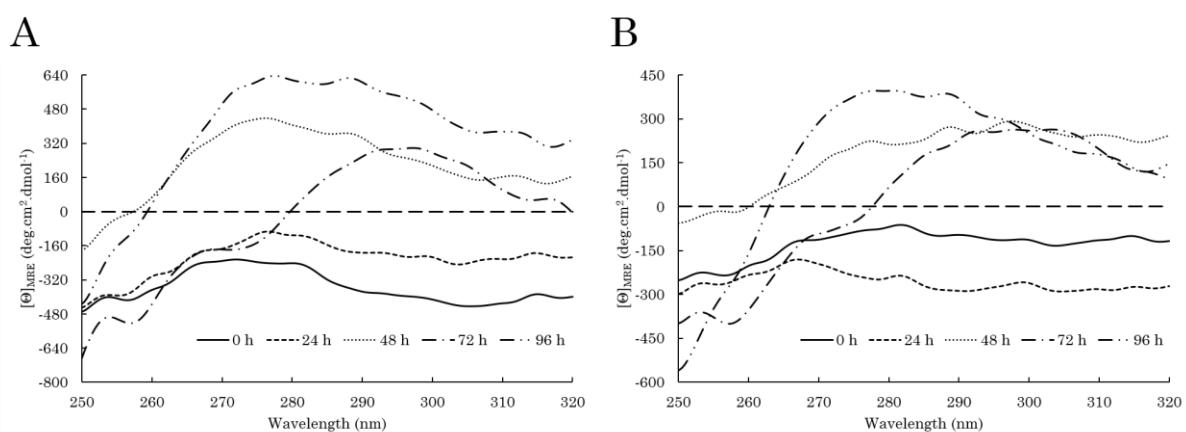


Figure S4 – Near-UV CD spectra of (A) C-TERb and (B) C-TERa ( $C_{\text{C-TER}} = 10\ \mu\text{M}$ ). after 0 h (solid line), 24 h (dashed line), 48 h (dotted line), 72 h (dash-dotted line), and 96 h (dash-double-dotted line) of incubation in TBS at  $\sim 20^\circ\text{C}$ .

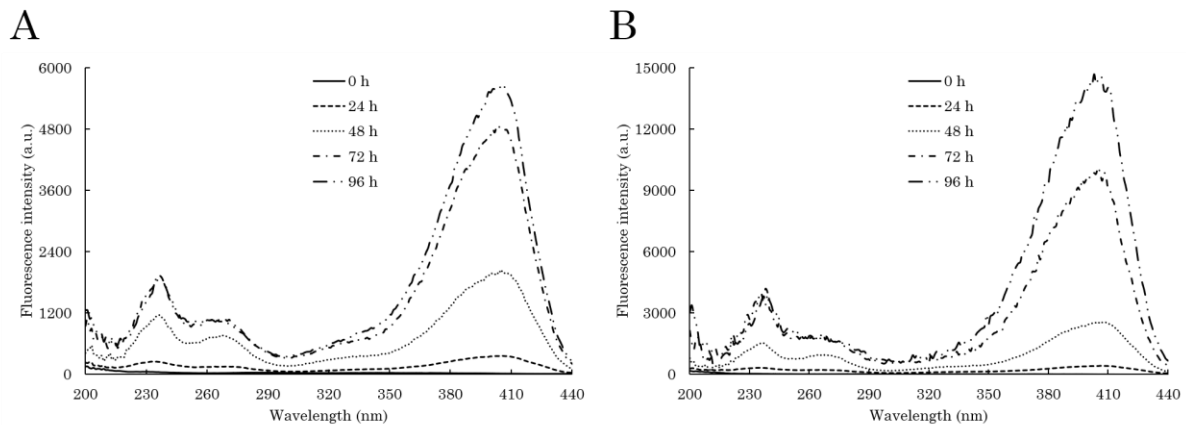


Figure S5 – dbAF excitation spectra ( $\lambda_{em} = 456$  nm,  $sw = 10$  nm) of (A) C-TERb and (B) C-TERa ( $C_{C-TER} = 10$   $\mu$ M) after 0 h (solid line), 24 h (dashed line), 48 h (dotted line), 72 h (dash-dotted line), and 96 h (dash-double-dotted line) of incubation in TBS at ~20 °C.

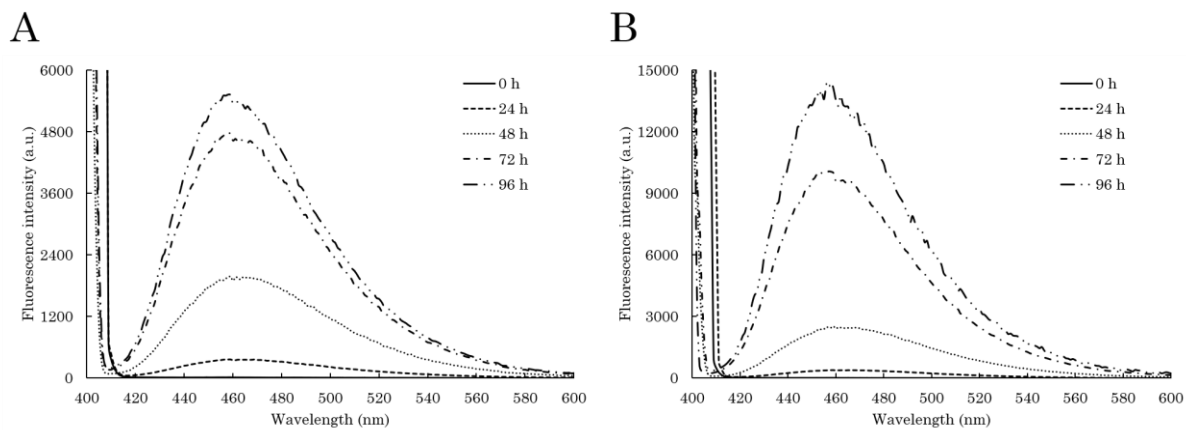


Figure S6 – dbAF spectra ( $\lambda_{ex} = 400$  nm,  $sw = 10$  nm) of (A) C-TERb and (B) C-TERa ( $C_{C-TER} = 10$   $\mu$ M) after 0 h (solid line), 24 h (dashed line), 48 h (dotted line), 72 h (dash-dotted line), and 96 h (dash-double-dotted line) of incubation in TBS at ~20 °C.

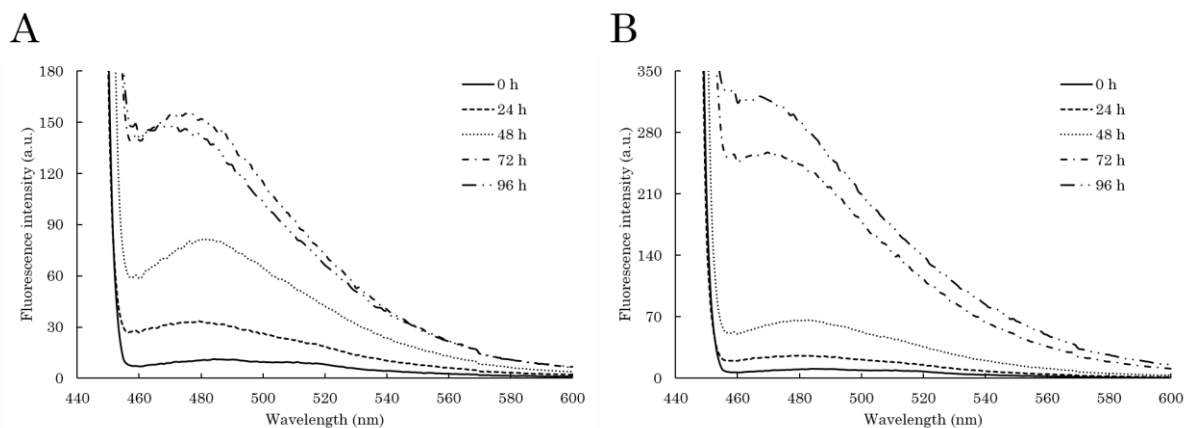


Figure S7 – ThT emission spectra ( $\lambda_{ex} = 440$  nm,  $sw = 10$  nm,  $C_{ThT} = 10$   $\mu$ M) of (A) C-TERb and (B) C-TERa ( $C_{C-TER} = 10$   $\mu$ M) after 0 h (solid line), 24 h (dashed line), 48 h (dotted line), 72 h (dash-dotted line), and 96 h (dash-double-dotted line) of incubation in TBS at ~20 °C.

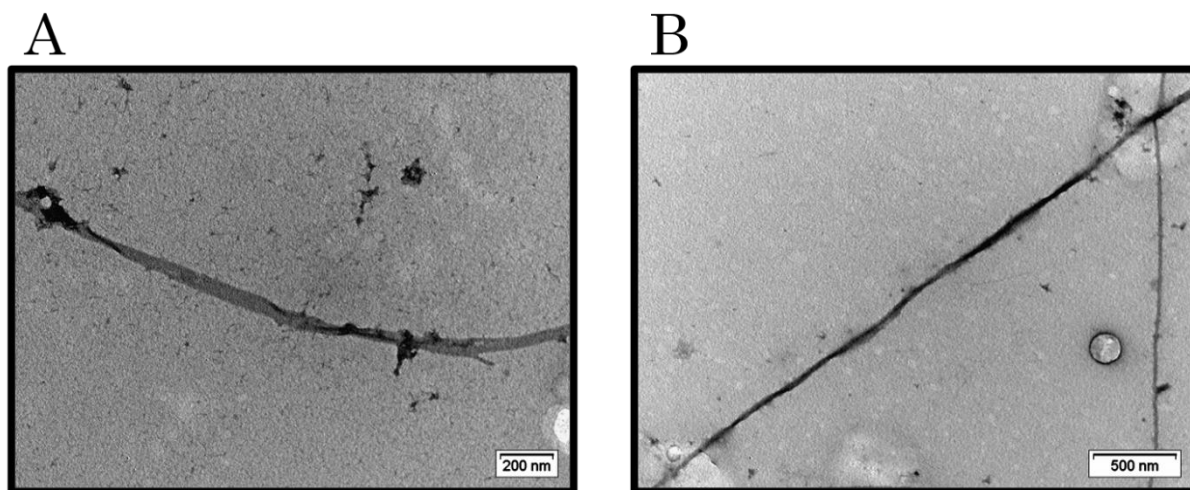


Figure S8 – Negatively stained TEM micrographs of (A) C-TERb and (B) C-TERa ( $C_{C-TER} = 10 \mu\text{M}$ ) thin twisted fibrils (TTFs) after 144 h (6 days) of incubation in TBS at  $\sim 20^\circ\text{C}$ . On each micrograph, the scale bar is indicated at the bottom right.

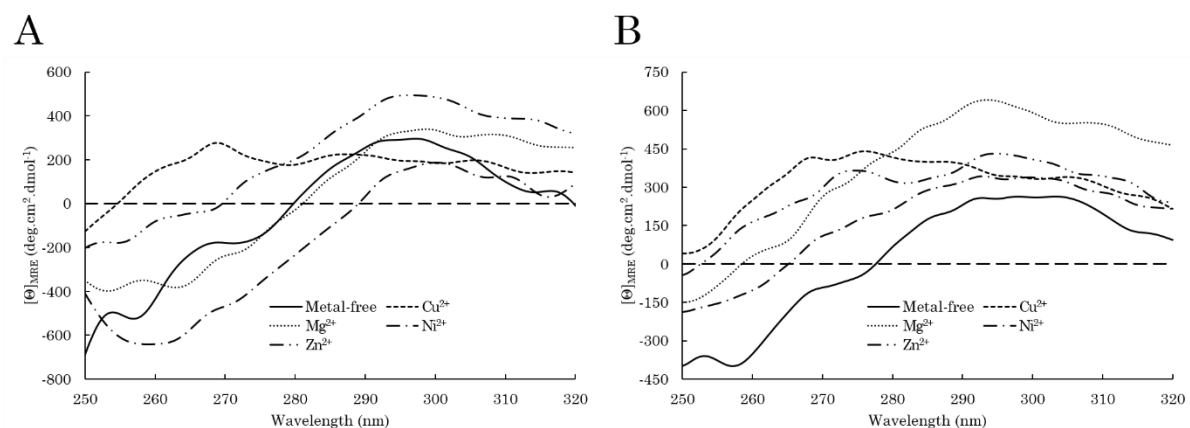


Figure S9 – Near-UV CD spectra of (A) C-TERb and (B) C-TERa ( $C_{C-TER} = 5 \mu\text{M}$ ) incubated in TBS at  $\sim 20^\circ\text{C}$  for 72 h without metal (solid line) and in the presence of  $\text{Cu}^{2+}$  (dashed line),  $\text{Mg}^{2+}$  (dotted line),  $\text{Ni}^{2+}$  (dash-dotted line), and  $\text{Zn}^{2+}$  (dash-double-dotted line) cations ( $C_{M^{2+}} = 100 \mu\text{M}$ ).

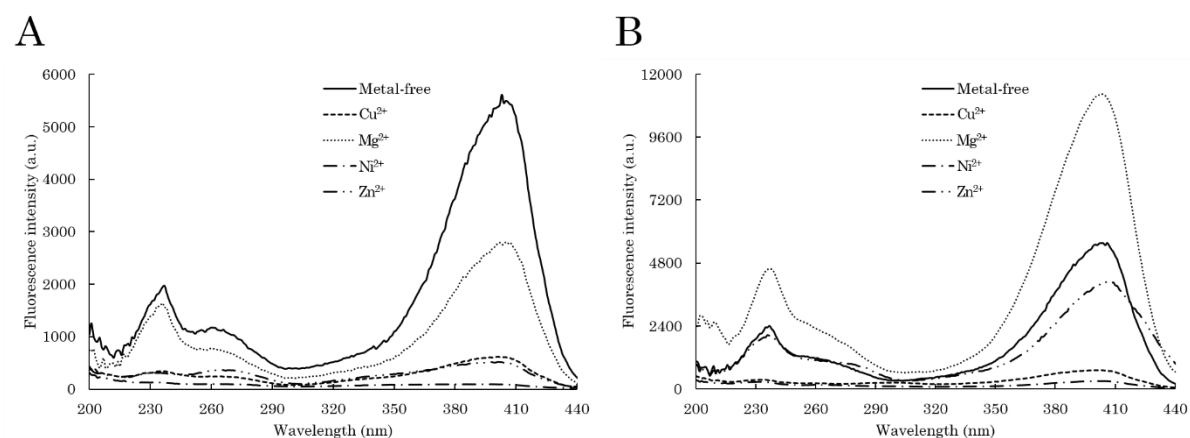


Figure S10 – dbAF excitation spectra ( $\lambda_{\text{em}} = 456 \text{ nm}$ ,  $\text{sw} = 10 \text{ nm}$ ) of (A) C-TERb and (B) C-TERa ( $C_{C-TER} = 5 \mu\text{M}$ ) incubated in TBS at  $\sim 20^\circ\text{C}$  for 72 h without metal (solid line) and in the presence of  $\text{Cu}^{2+}$  (dashed line),  $\text{Mg}^{2+}$  (dotted line),  $\text{Ni}^{2+}$  (dash-dotted line), and  $\text{Zn}^{2+}$  (dash-double-dotted line) cations ( $C_{M^{2+}} = 100 \mu\text{M}$ ).

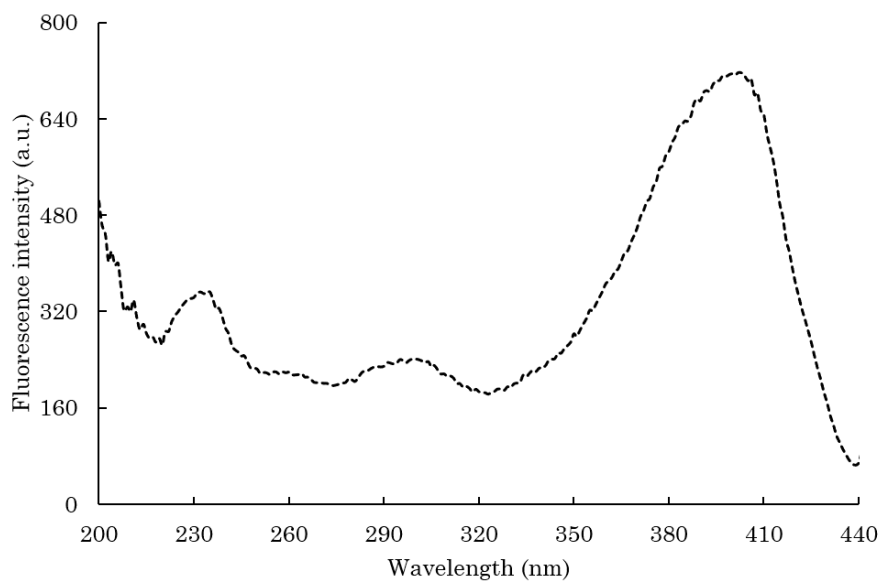


Figure S11 – dbAF excitation spectrum ( $\lambda_{\text{em}} = 456 \text{ nm}$ ,  $\text{sw} = 10 \text{ nm}$ ) of C-TERa ( $C_{\text{C-TERa}} = 5 \mu\text{M}$ ) incubated in TBS at  $\sim 20^\circ\text{C}$  for 72 h in the presence of  $\text{Cu}^{2+}$  ( $C_{\text{Cu}^{2+}} = 100 \mu\text{M}$ ).

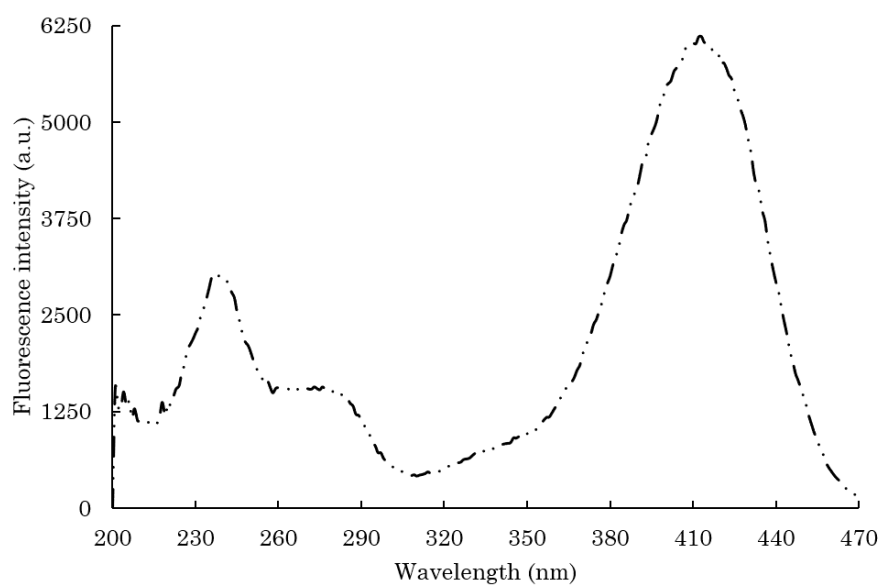


Figure S12 – dbAF excitation spectrum ( $\lambda_{\text{em}} = 490 \text{ nm}$ ,  $\text{sw} = 10 \text{ nm}$ ) of C-TERa ( $C_{\text{C-TERa}} = 5 \mu\text{M}$ ) incubated in TBS at  $\sim 20^\circ\text{C}$  for 72 h in the presence of  $\text{Zn}^{2+}$  ( $C_{\text{Zn}^{2+}} = 100 \mu\text{M}$ ).

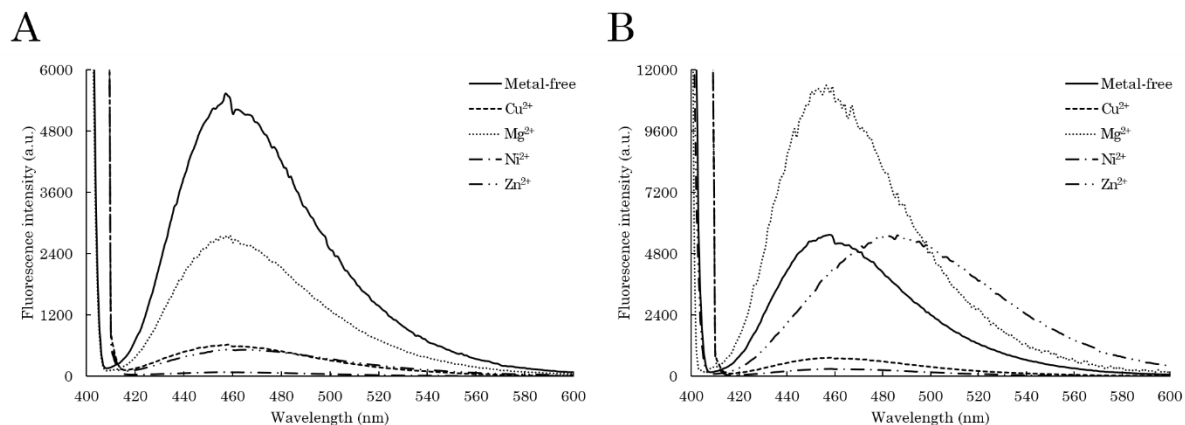


Figure S13 – dbAF spectra ( $\lambda_{\text{ex}} = 400$  nm,  $\text{sw} = 10$  nm) of (A) C-TERb and (B) C-TERa ( $C_{\text{C-TER}} = 5$   $\mu\text{M}$ ) incubated in TBS at  $\sim 20$   $^{\circ}\text{C}$  for 72 h without metal (solid line) and in the presence of  $\text{Cu}^{2+}$  (dashed line),  $\text{Mg}^{2+}$  (dotted line),  $\text{Ni}^{2+}$  (dash-dotted line), and  $\text{Zn}^{2+}$  (dash-double-dotted line) cations ( $C_{\text{M}^{2+}} = 100$   $\mu\text{M}$ ).

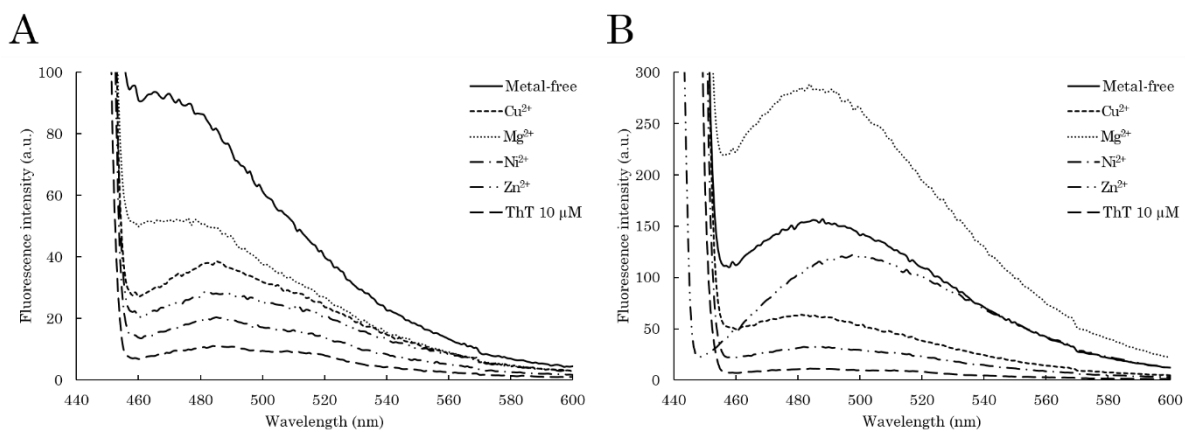


Figure S14 – ThT emission spectra ( $\lambda_{\text{ex}} = 440$  nm,  $\text{sw} = 10$  nm,  $C_{\text{ThT}} = 10$   $\mu\text{M}$ ) of (A) C-TERb and (B) C-TERa ( $C_{\text{C-TER}} = 5$   $\mu\text{M}$ ) incubated in TBS at  $\sim 20$   $^{\circ}\text{C}$  for 72 h without metal (solid line) and in the presence of  $\text{Cu}^{2+}$  (dashed line),  $\text{Mg}^{2+}$  (dotted line),  $\text{Ni}^{2+}$  (dash-dotted line), and  $\text{Zn}^{2+}$  (dash-double-dotted line) cations ( $C_{\text{M}^{2+}} = 100$   $\mu\text{M}$ ). The spectrum of ThT 10  $\mu\text{M}$  alone in TBS is represented by the long-dashed line.



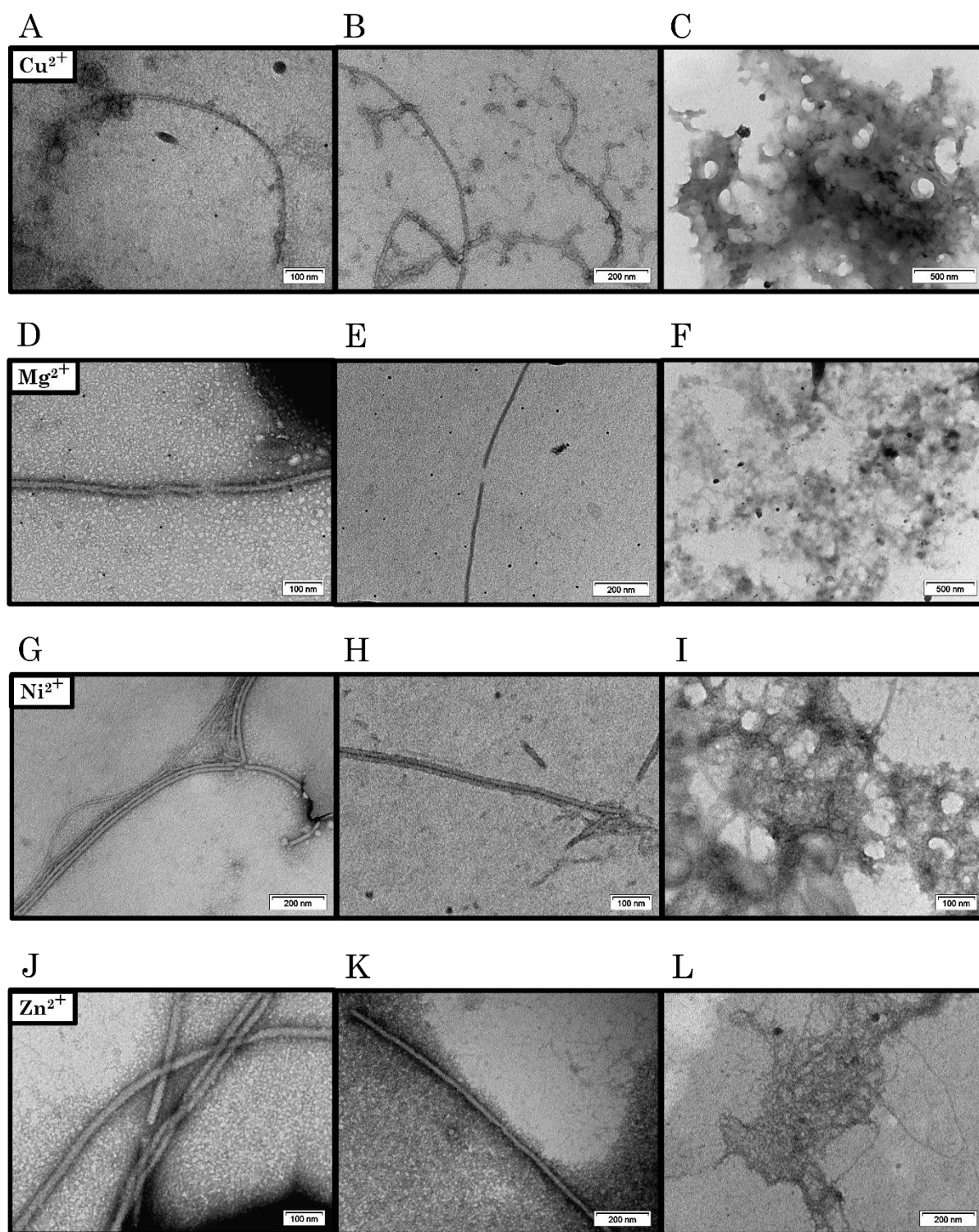


Figure S15 – Negatively stained TEM micrographs of C-TERb ( $C_{\text{C-TERb}} = 5 \mu\text{M}$ ) incubated for 144 h (6 days) in TBS at  $\sim 20^\circ\text{C}$  in the presence of (A, B, C)  $\text{Cu}^{2+}$ , (D, E, F)  $\text{Mg}^{2+}$ , (G, H, I)  $\text{Ni}^{2+}$ , and (J, K, L)  $\text{Zn}^{2+}$  cations ( $C_{\text{M}^{2+}} = 100 \mu\text{M}$ ). Amorphous phases are observed in each condition (C, F, I, L). On each micrograph, the scale bar is indicated at the bottom right.

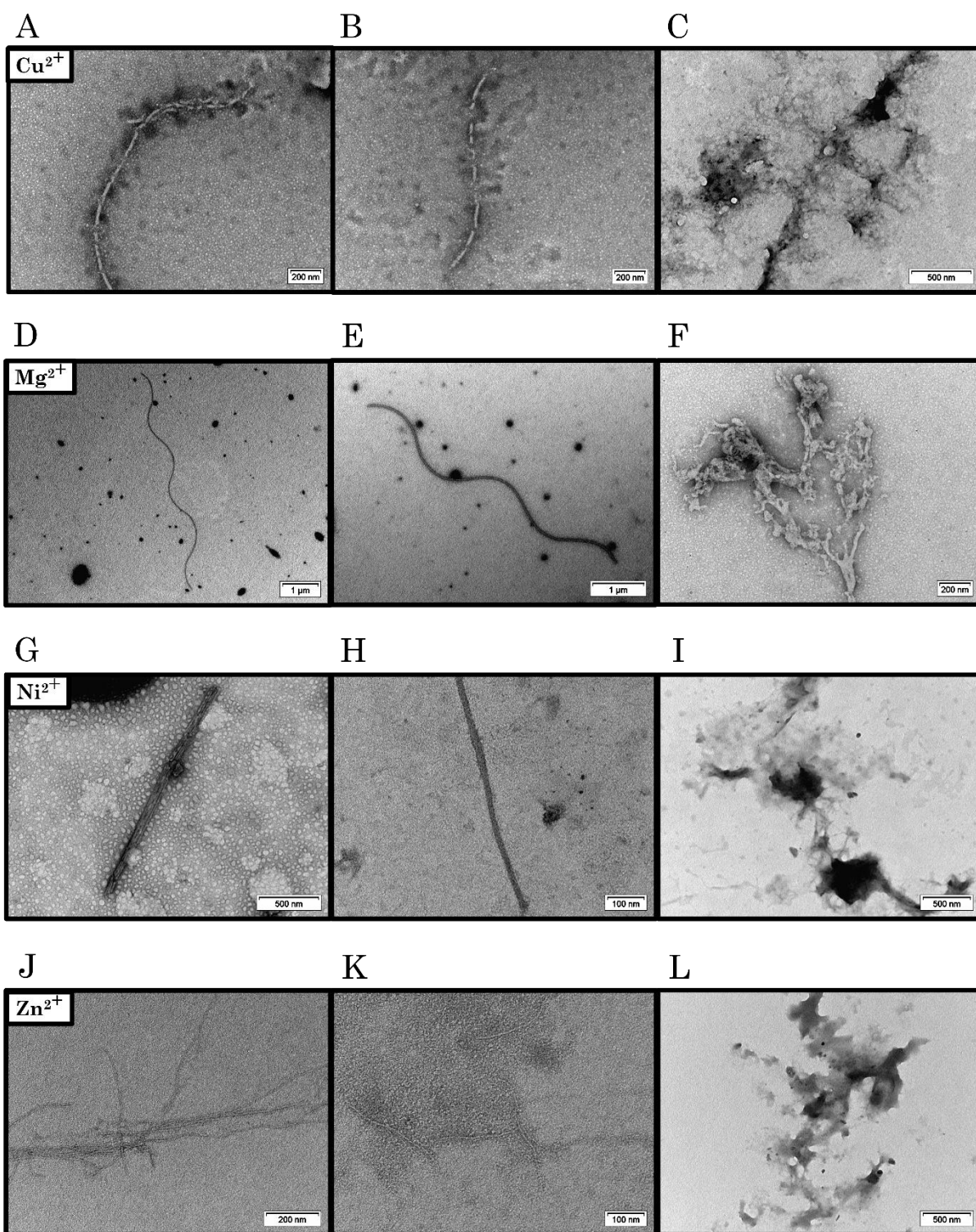


Figure S16 – Negatively stained TEM micrographs of C-TERa (C<sub>C-TERa</sub> = 5 μM) incubated for 144 h (6 days) in TBS at ~20 °C in the presence of (A, B, C) Cu<sup>2+</sup>, (D, E, F) Mg<sup>2+</sup>, (G, H, I) Ni<sup>2+</sup>, and (J, K, L) Zn<sup>2+</sup> cations (C<sub>M²⁺</sub> = 100 μM). Amorphous phases are observed in each condition (C, F, I, L). On each micrograph, the scale bar is indicated at the bottom right.